

## DYNAMIC STABILITY DERIVATIVES OF A MANUEVERING COMBAT AIRCRAFT MODEL

**Mehmet ALTUN**

Hava Harp Okulu Yesilyurt-ISTANBUL  
m.altun@hho.edu.tr

**İbrahim İYİGÜN**

Hava Kuvvetleri Pl.P.Bşk.-Ankara  
iiygün@hvkk.tsk.mil.tr

### ÖZET

*Bu deneysel çalışmanın amacı, salınım yapmakta olan jenerik bir savaş uçağı modelinin 'Forced Oscillation' tekniğı kullanılarak statik ve dinamik kararlılık türevlerinin Ankara Rüzgar Tüneli'nde bulunmasıdır. Salınım testleri için kullanılan model AGARD, Standart Dinamik Modelidir. Bu model bir çok NATO ülkesinde farklı ölçüm teknikleri kullanılarak rüzgar rünellerinin verifikasyonu için üretilmiştir. Bu model üzerine etki eden aerodinamik yükler, ölçüm sisteminin en önemli parçası olan beş bileşenli balans tarafından ölçülmektedir. Bu makalede çalışmada kullanılan; deney düzeneğı, hareket kontrol ve ölçüm sistemi ile statik ve dinamik test sonuçları sunulmuştur.*

**Anahtar kelimeler:** Dinamik kararlılık türevi, Standart dinamik model, salınım

### ABSTRACT

*The purpose of this experimental study presented in this paper is to measure the dynamic stability derivatives of a generic combat aircraft model in the Ankara Wind Tunnel by using the direct forced oscillation technique. The model, which is used for the oscillatory tests is known as the AGARD, Standard Dynamic Model (SDM) and is manufactured as a generic combat aircraft model to verify different measurement techniques in various wind tunnels of NATO countries. The aerodynamic loads acting on the model are measured with a five component internal strain gauge balance placed inside the oscillating model. The paper presents the experimental set-up used to create the oscillatory motion in pitch for the model and the related motion control and the data acquisition units to measure the dynamic loads, and discussed the results of the measurements.*

**Keywords:** Dynamic stability derivative, Standard dynamic model, Oscillation

## 1. INTRODUCTION

The performance requirements of today's fighter aircraft have tremendously increased in terms of their capabilities of flying at high angles of attack and performing rapid, maneuvers under adverse conditions. In parallel, aircraft control techniques have also improved which has led to highly maneuverable and agile aircraft. At high angles of attack, unusual combinations of accelerations and angular rates are met. For this reason, the experimental approach has become an essential tool for determining the aircraft's dynamic stability and therefore many wind tunnel testing techniques are developed to analyze these nonlinearities of high performance aircraft.

The purpose of this experimental investigation is to perform direct forced oscillation tests to measure the static and dynamic stability derivatives of a maneuvering generic combat aircraft model in the Ankara Wind Tunnel (AWT). Forced oscillation

technique is one of the methods used to measure the dynamic stability derivatives. Another well known technique is the so-called rotary technique.

Direct forced oscillation technique is based on the principle of oscillating the aircraft model around its center of gravity by push-rod-crank mechanism from its tail at constant amplitude in single degree of freedom. So the relationship between the aerodynamic

forces and the primary motion is established. Experiments, in which the primary oscillation takes place in different degrees of freedom, yields various dynamic stability derivatives.

## 2. EXPERIMENTAL SET-UP

### 2.1 The Standard Dynamic Model (SDM):

The standard dynamic model (SDM) is a calibration model which is first introduced by the National

Research Council of Canada (NRC) / Institute for Aerospace Research (IAR) in 1978, specifically designed for dynamic tests[1].

The standard dynamic model (SDM) used in the tests is shown in Figure 1[4]. The material used for the model is mainly aluminum alloy. The wing surface is trapezoidal in shape with a  $40^{\circ}$  sweep angle. The geometrical dimensions of the SDM are given in Table 1 [5].

**Table 1.** Main Dimensions of the SDM

Length	0.943 m
Span	0.609 m
Mean Aerodynamic Chord	0.220 m
Wing Area	$0.117 \text{ m}^2$
Fuselage Diameter	0.135 m
Ogive Ratio	3:1
Weight(without balance and adaptor)	8 kg.

**2.2 Description of the Apparatus:**

In order to perform the static and the dynamic tests on the aircraft model a servo mechanical system is designed, manufactured and installed in the Ankara Wind Tunnel (AWT). The system generates simple harmonic oscillatory motions for the Standard Dynamic Model (SDM) [4] with only one rotational degree of freedom in the pitch plane.

The general layout of the experimental set up is shown in Figure 2. The driving unit that generates the simple harmonic motion of the model in the pitch plane is placed under the floor of the wind tunnel test section. The driving unit is powered by means of a DC servo motor mounted on the adjustable arm (13) at location (17) and is linked to the oscillating vertical push rod (11) which oscillates the model from the rear of its fuselage by an eccentric crank-rod mechanism (16).

The amplitude of oscillations for the model is adjusted by setting the flywheel's (16) eccentricity radius, which can be changed within a range of 50 mm, causing  $\pm 5^{\circ}$  of pitch oscillations in amplitude for the model. The oscillation frequency of the model, whose upper limit is 5 Hz, is set by the rotational speed of the DC servomotor.

The angle of attack mechanism of the experimental set up enables to change the angle of attack within a range of  $-15^{\circ}$  to  $+45^{\circ}$ . The sideslip angle of the model can be adjusted from  $-45^{\circ}$  to  $+45^{\circ}$ . Both the angle of attack and the sideslip angle adjustments are done manually.

**2.3 Measurement System;**

The measurement system used to measure the stability derivatives is composed of a motion generation and control unit, an internal balance system with force transducers, a signal conditioning unit, and a data

acquisition unit (A/D Conversion) which are all interfaced to a personnel computer to control, store, display and analyze the parameters collected during the experiments.

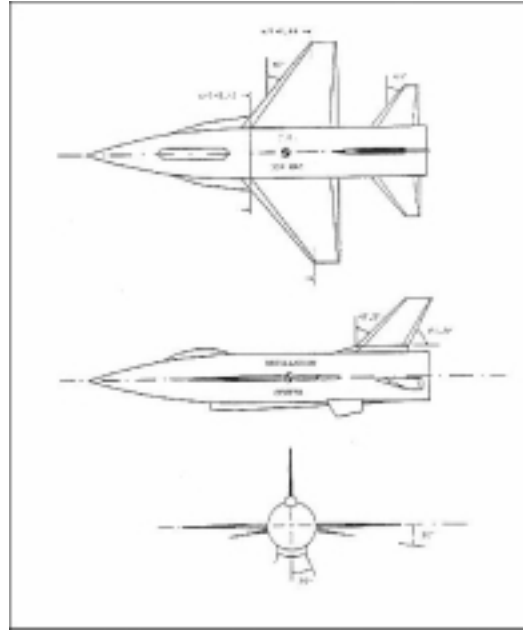


**Figure 1.** The geometry of the Standard Dynamic Model used in the tests.

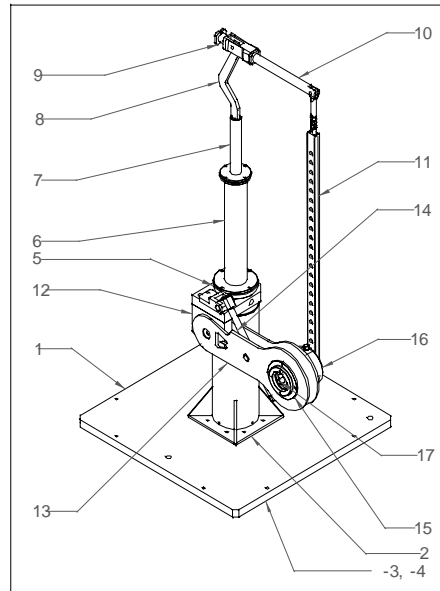


**Figure 2.** Parts of the AWT Test Rig (Perspective View)

**2.3.1 Motion Generation and Control Unit:**

The motion generation and control unit is composed of a DC servomotor (6SM57S-3000 produced by Kollmorgen, in Germany), motor resolver and the power driver. The rotational motion of the servomotor

is converted into simple harmonic motion of the model by means of the eccentric arm (16) and the oscillating vertical push rod (11).

The speed of the servomotor is controlled by the driver unit. The frequency of oscillations of the model is set directly by the rotational speed of the DC servomotor.

**2.3.2 The Internal Balance:**

The five component internal balance is the heart of the measurement system for the present experimental investigations. The internal balance is connected to the model in such a way that it permits the measurement of the driving torque due to the mechanical and the aerodynamic loads on the oscillating model. The technical drawing of the five-component internal balance system is given in Figure 3.

Although the internal balance, used is a five component balance, designed to measure, the pitch, the roll and the yaw moments as well as the normal and the side forces with the exception of the axial force, during the present experiments only three of these components are measured due to the limitations in the number of simultaneous sampling channels of the data acquisition system used. These are the normal force, the pitch and the roll moments. Hence, the original 5 x 5 calibration matrix of the internal balance is reduced to 3 x 3 matrix to adapt to the present situation. The reduced calibration matrix is given as[2].

$$\begin{bmatrix} L \\ Z \\ M \end{bmatrix} = \frac{2000}{G * V_0} \begin{bmatrix} 0.04558 & -0.00396 & -0.00344 \\ 0.00147 & 0.84753 & -0.01838 \\ 0.00039 & 0.00023 & 0.03897 \end{bmatrix} \begin{bmatrix} VL \\ VZ \\ VM \end{bmatrix} \quad (1)$$

where L, Z, M, are the rolling moment, the normal force and the pitching moment respectively. G is the actual gain of the amplifier, V<sub>0</sub> is the voltage supply of the internal balance. VL, VZ, VM are the balance voltage outputs for the rolling moment, the normal force and the pitching moment respectively. In the present tests, the actual gain of the amplifier, G, is set to 2000 and the voltage supply of the internal balance, V<sub>0</sub>, is set to 9 Volts.

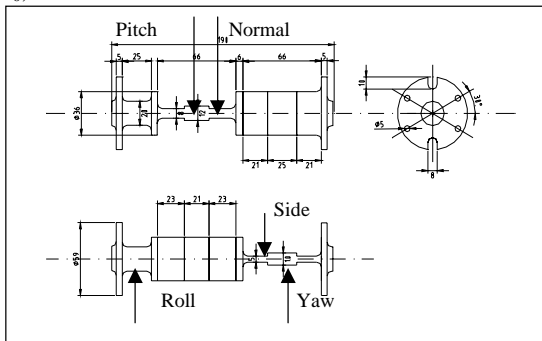


**Figure 3. Technical Drawing of the Internal Balance**

**2.3.3 Signal conditioning Unit and Data Acquisition Card:**

In general transducers generate signals that must be conditioned so that it can be acquired reliably and accurately by the data acquisition device. The signal conditioning unit used includes amplification, filtering, electrical isolation, multiplexing and completing the bridge of transducers to produce high level signals for the data acquisition device. The National Instrument’s SCXI-1120 and SCXI-1140 cards are chosen as signal conditioning units for the internal balance measurements. These signal conditioning modules are placed in a 12-slot chassis. For data acquisition the National Instrument’s PCI-6024E card is used.

**2.3.4 Measurement System Software:**

After interfacing all the components of the measurement system, the implementation for the desired operations of the dynamic testing is achieved by means of the “Labview” programming software. Labview® is a high level programming language which is suitable for the static and the dynamic test programming required for the present experiments. This programming language also allows to create user interfaces for interactive monitoring of the control programmes. The measurement program controls the process of the data acquisition and performs the analysis of the acquired data.

**3. RESULTS AND CONCLUSIONS**

This part deals with the results of the static and dynamic tests and their correlation with the previous results obtained from other test facilities[6]. The results are presented as functions of angle of attack. In the tests, the effects of frequency of oscillations and their amplitudes as well as the wind speed are investigated.

The experiments are performed in the 8’ x 10’ low-speed, closed circuit Ankara Wind Tunnel (AWT)[7]. The results obtained include a complete set of derivatives due to oscillation in pitch for the basic configuration of the model, BWLVH (B-Body, W-Wing, L-LEX, V-Vertical tail, H-Horizontal tail). Comparison of the present results with the previous results obtained in other test facilities such as NAE (National Aeronautical Establishment, of Canada) and TPI, (Politecnico di Torino, Italy) are also presented. However, the experimental results will be presented in two parts. In the first part the static results and in the second part the dynamic results will be presented

**3.1 Results for Static Tests:**

Static tests are performed with the model fixed at a certain angle of attack without oscillating the model and under the following test conditions:

Velocity : 20, 30, 40 m/s  
 Angle of attack : from  $-6^{\circ}$  to  $30^{\circ}$   
 Angle of sideslip :  $0^{\circ}$   
 Model Configuration : BWLVH

The data reduction process for the static tests is based on the taking the average value of the data in order to calculate the coefficients. The results obtained for the static coefficients of  $C_l$ ,  $C_z$ , and  $C_m$  at a speed of 40 m/s are presented in Figures 4 to 6. In order to check the repeatability of the tests, measurements are repeated three times for each case. In general, the agreement between the three sets of data was good except for the rolling moment,  $C_l$ . The values for the rolling moment are very small and therefore are not very significant as can be seen in Figure 4.

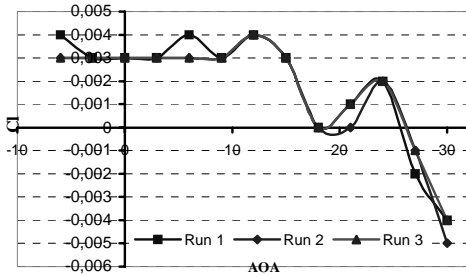


**Figure 4.** Variation of the static roll moment coefficient  $C_l$  with angle of attack at  $V=40$  m/s (data repeatability)

The trend of normal force coefficient,  $C_z$ , is presented in Figure 5 at a speed of 40 m/s. From the figure it is clear that the normal force coefficient exhibits a linear variation up to  $\alpha=18^{\circ}$ , where the wing-stall occurs. The resulting loss of lift due to this stall is also observed in the kink of the  $C_z$  curve around  $\alpha=18^{\circ}$ .

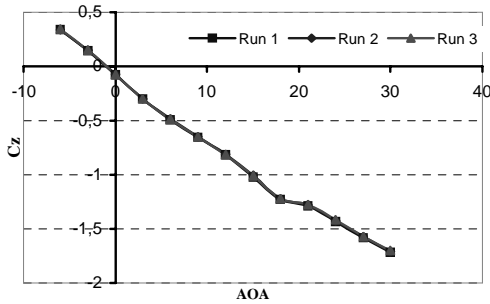


**Figure 5.** Variation of the static normal force coefficient  $C_z$  with angle of attack at  $V=40$  m/s (data repeatability)

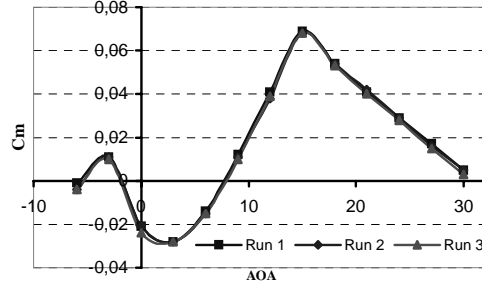


**Figure 6.** Variation of the static pitching moment coefficient  $C_m$  with angle of attack at  $V=40$  m/s (data repeatability)

The variation of the pitching moment coefficient,  $C_m$  with AOA, can be seen in Figure 6 at a speed of 40 m/s. The pitching moment curve increases linearly with angle of attack in the range from  $-6^{\circ}$  to  $-3^{\circ}$  and decreases in the interval of  $-3^{\circ}$  to  $0^{\circ}$ . The pitching moment curve is linear from  $\alpha=5^{\circ}$  up to  $\alpha=15^{\circ}$  and between  $0^{\circ}$  and  $5^{\circ}$  it goes through a minimum value. At  $\alpha=15^{\circ}$ , the pitching moment coefficient  $C_m$  attains a peak value. After this peak,  $C_m$  starts to decline linearly with angle of attack up to  $\alpha=30^{\circ}$ . It appears that separation on the horizontal stabilizer is delayed by the downwash of the wing so that the normal force slope of the stabilizer is kept at relatively high values due to the effectively lower angle of attack. Thus, when the wing  $C_z$  is reduced by tip stalling above  $\alpha=18^{\circ}$ , a stabilizing pitching moment results. The favorable effect of the wing downwash is maintained up to about  $30^{\circ}$  which was also the case observed in reference[8].

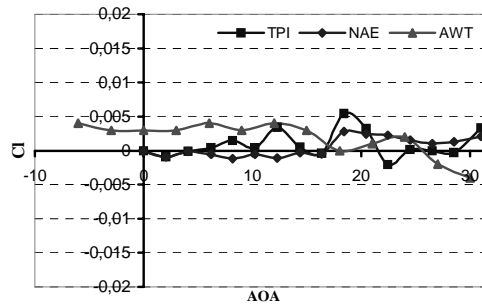


**Figure 7.** Variation of the static coefficient  $C_l$  with angle of attack and its comparison with results obtained in other test facilities.

The primary aim of the present investigations was to evaluate the reliability of the tests done with the same model in different wind tunnels. The static test results of the AWT are generally in good agreement with those obtained in other test facilities (TPI, NAE). This can be seen in Figures 7, 8, 9 for the rolling moment, the normal force and the pitching moment coefficients respectively. Differences become evident for  $\alpha$  larger than  $25^{\circ}$  for the longitudinal coefficients  $C_z$  and  $C_m$  (Figures 8 and 9).

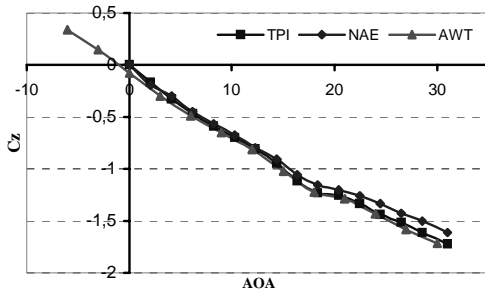


**Figure 8.** Variation of the static coefficient  $C_z$  with angle of attack and its comparison with results obtained in other test facilities.

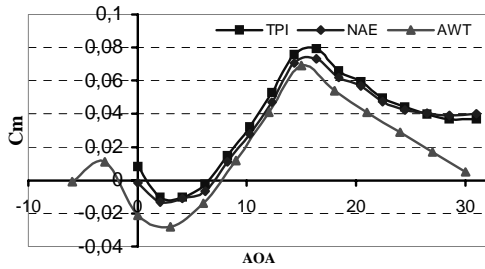


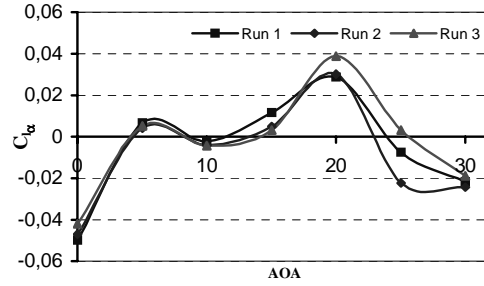
**Figure 9.** Variation of the static coefficient  $C_m$  with angle of attack and its comparison with results obtained in other test facilities.

### 3.2 Results for Dynamic Tests:

The dynamic tests are conducted with the model oscillating under the following test conditions:

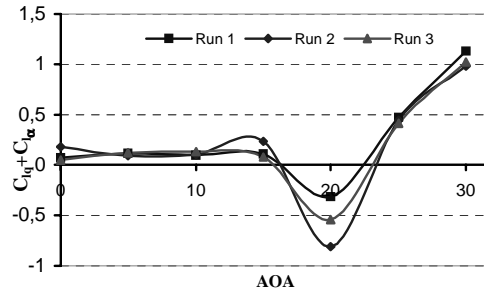
- Velocity : 20, 30, 40 m/s
- Angle of attack : from  $0^{\circ}$  to  $30^{\circ}$
- Angle of sideslip :  $0^{\circ}$
- Mode of motion : Pitch oscillation
- Amplitude :  $1^{\circ}, 2^{\circ}$
- Frequency : 1, 2 Hz
- Model Configuration : BWLVH

The dynamic testing procedure is based on the measurement of the external loads acting on the model oscillating with respect to its center of gravity. This primary motion must be harmonic, so that, with the assumption that the system behavior is linear. The purpose of the oscillatory tests was to get the stiffness and the damping derivatives for the rolling moment,  $C_l$ , the normal force,  $C_z$ , and the pitching moment,  $C_m$ . The stiffness derivative for the roll moment,  $C_{l\alpha}$  (Figure 10) is very small and remains around zero in the total range of AOA investigated.



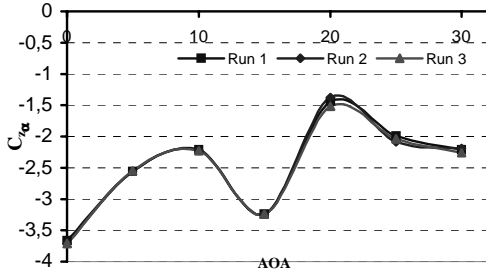
**Figure 10.** The Stiffness Derivative of roll moment  $C_{l\alpha}$  at  $V = 30\text{m/s}$ ,  $f = 2\text{Hz}$ ,  $\theta = \pm 1^{\circ}$  (data repeatability)

A similar behavior is also observed for the damping derivative of the roll moment,  $C_{lq} + C_{l\dot{\alpha}}$  (Figure 11) for  $\alpha < 15^{\circ}$ . For  $\alpha > 15^{\circ}$ , the damping derivatives of the roll moment decreases to reach a minimum amount  $20^{\circ}$  and then increases steadily up to  $\alpha = 30^{\circ}$ . As expected, the rolling moment derivatives, which is a cross-coupling derivative for pitch oscillations, are very small at zero sideslip angle for  $\alpha < 15^{\circ}$ . Above this angle of attack, flow separation and its resulting asymmetries cause both the damping and the stiffness coefficients of the roll moment to change considerably.



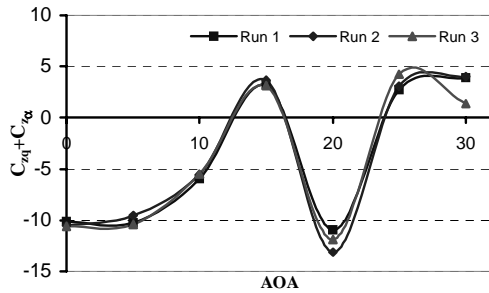
**Figure 11.** The Damping Derivative of roll moment  $C_{lq} + C_{l\dot{\alpha}}$  at  $V = 30\text{m/s}$ ,  $f = 2\text{Hz}$ ,  $\theta = \pm 1^{\circ}$  (data repeatability)

Figure 12 shows the variation of the stiffness derivative  $C_{z\alpha}$  and Figure 13 shows that of the damping derivative  $C_{zq} + C_{z\dot{\alpha}}$  of the normal force coefficient  $C_z$  with respect to  $\alpha$ .



**Figure 12.** The Stiffness Derivative of the normal force,  $C_{z\alpha}$  at  $V = 30\text{m/s}$ ,  $f = 2\text{Hz}$ ,  $\theta = \pm 1^\circ$  (data repeatability)

The normal force damping derivative  $C_{zq} + C_{z\dot{\alpha}}$  at zero sideslip angle, initially peaks at  $\alpha=15^\circ$ , after which a sharp drop occurs to reach a minimum value at  $\alpha=20^\circ$  as can be seen in Figure 13. Beyond this point the damping rises to a steady level at  $\alpha=25^\circ$ .  $C_{zq} + C_{z\dot{\alpha}}$  exhibits an opposing trend to that of the stiffness derivative  $C_{z\alpha}$ , such that its negative and positive peaks are approximately at the same angles of attack as in the damping case, namely at  $\alpha=15^\circ$  and  $20^\circ$  respectively.



**Figure 13.** The Damping Derivative of the normal force  $C_{zq} + C_{z\dot{\alpha}}$  at  $V = 30\text{m/s}$ ,  $f = 2\text{Hz}$ ,  $\theta = \pm 1^\circ$  (data repeatability)

The variation of the stiffness derivative of the pitching moment,  $C_{m\alpha}$  is presented in Figure 14. The stiffness derivative  $C_{m\alpha}$  rises linearly and peaks at  $\alpha \approx 10^\circ$ . It then reaches an asymptotic value starting at  $\alpha=15^\circ$ .

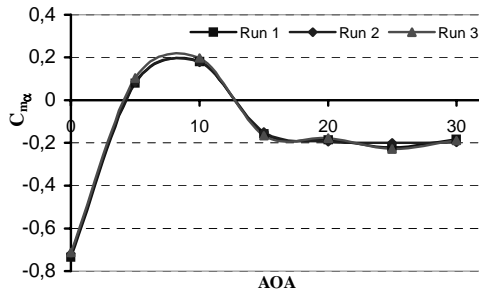


**Figure 14.** The Stiffness Derivative of the pitching moment  $C_{m\alpha}$  at  $V = 30\text{m/s}$ ,  $f = 2\text{Hz}$ ,  $\theta = \pm 1^\circ$  (data repeatability)

The variation of the damping derivative  $C_{mq} + C_{m\dot{\alpha}}$  is presented in Figure 15. Initially the damping derivative  $C_{mq} + C_{m\dot{\alpha}}$  shows a steady behavior which rises and peaks at  $\alpha=20^\circ$  after which it starts to decrease.

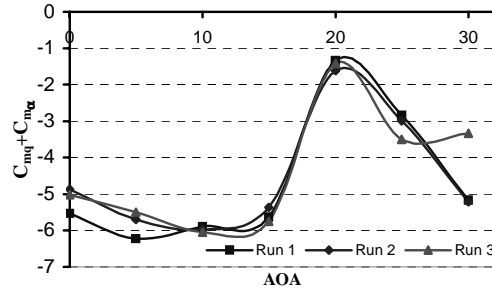


**Figure 15.** The Damping Derivative of the pitching moment  $C_{mq} + C_{m\dot{\alpha}}$  at  $V = 30\text{m/s}$ ,  $f = 2\text{Hz}$ ,  $\theta = \pm 1^\circ$  (data repeatability)

Comparison of the rolling moment stiffness and damping coefficient variations with respect to angle of attack with those obtained in other wind tunnel facilities can be seen in Figures 16 and 17 respectively. The value of the stiffness coefficient  $C_{l\alpha}$  (Figure 16) is very small and remains around zero in the complete range of angle of attacks studied. A similar behavior is also observed for the damping derivative  $C_{lq} + C_{l\dot{\alpha}}$  variation with respect to angle of attack (Figure 17).

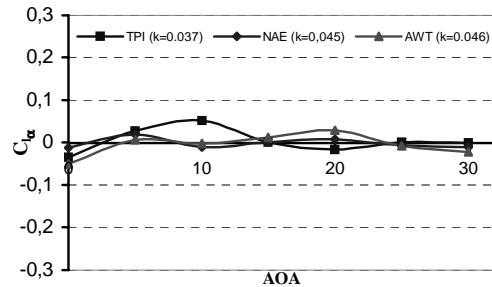


**Figure 16.** Comparisons of  $C_{l\alpha}$  coefficient measurements with results obtained in other test facilities

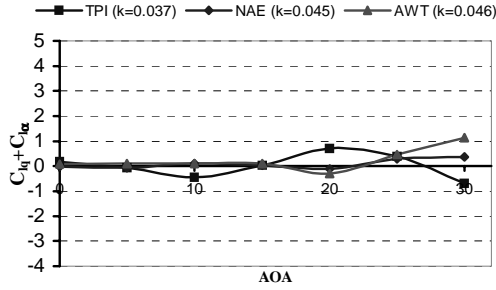


Figure 17. Comparisons of  $C_{lq} + C_{l\dot{\alpha}}$  coefficient measurements with results obtained in other test facilities

In Figures 18 and 19 the normal force stiffness and damping coefficients variation with angle of attack are compared with the results obtained in Politecnico di Torino (TPI). The results exhibit similar trends for but for  $\alpha < 20^\circ$ , values of  $\alpha$  larger than  $20^\circ$  the damping coefficients measured in AWT and TPI show different behaviors.

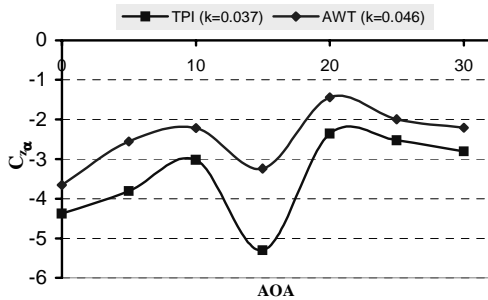


Figure 18. Comparisons of  $C_{z\alpha}$  coefficient measurements with results obtained in other test facilities

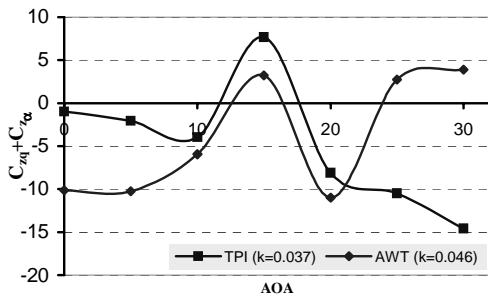


Figure 19. Comparisons of  $C_{zq} + C_{z\dot{\alpha}}$  coefficient measurements with results obtained in other test facilities

The stiffness and the damping coefficients for the pitching moment are compared with those obtained in TPI and NAE in Figures 20 and 21 respectively. Differences in the measured values are evident in the

whole range of angle of attacks considered. However the trends are observed to be similar. The differences observed between the present test results and those of the other test facilities can be attributed to the particular characteristics of each experimental set-up used; such as differences in the suspension systems, characteristics of the wind tunnels effects of model blockage and interferences, flow asymmetries caused by the support systems, etc.

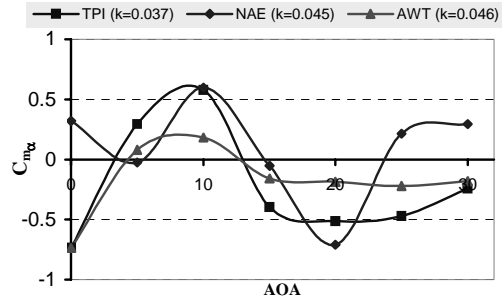


Figure 20. Comparisons of  $C_{m\alpha}$  coefficient measurements with results obtained in other test facilities

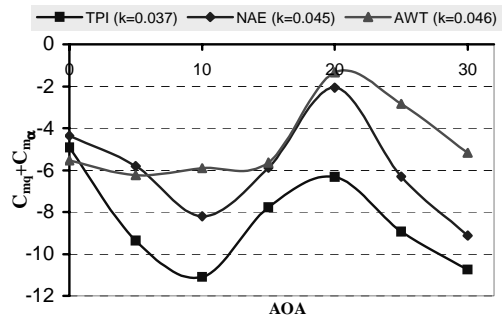


Figure 21. Comparisons of  $C_{mq} + C_{m\dot{\alpha}}$  coefficient measurements with results obtained in other test facilities

4. DISCUSSIONS

This experimental investigation is an attempt to show the feasibility of experiments using the forced oscillation technique in the Ankara Wind Tunnel to determine the dynamic stability derivatives. Comparisons of the present results with the results obtained in other test facilities such as NAE (National Aeronautical Establishment, of Canada) and TPI, (Politecnico di Torino, Italy) show good agreement.

In Figure 5, the position observed for the kink in the slope of the normal force coefficient  $C_z$  is compared with the results of other facilities and is found to be in good agreement within the proximity of  $\alpha = 18^\circ$  for zero sideslip angle. Differences become noticeable for values of  $\alpha$ , larger than  $25^\circ$  for the coefficients  $C_z$  and  $C_m$  (Figures 5 and 6). The values obtained for  $C_l$  are

very small, but consistent with the measurements done in other test facilities.

In dynamic tests, the effects of the frequency and the amplitude of oscillations are investigated at different angles of attack over a range of  $0^0$  to  $30^0$ . Good repeatability of the dynamic test measurements can be seen from Figures 12 to 17 except for the rolling moment damping coefficients,  $C_{lq} + C_{l\dot{\alpha}}$ . The highly nonlinear nature of aircraft's stability characteristics at high  $\alpha$  is once again demonstrated in the dynamic test results shown in Figures 10 to 15. The direct derivatives due to oscillation in pitch (i.e. pitching derivatives) are highly nonlinear with  $\alpha$  at zero sideslip angle.

The differences observed in figures 18, 19, 20, and 21 between the present measurements and those obtained in other wind tunnels for the stiffness and the damping coefficients can be attributed to the fact that during the experiments the center of gravity of the model and the center of oscillation were not coincident. The C.G. of the model was located forward of the center of oscillation. This inconsistency in the C.G. and oscillation center was much more evident and pronounced in the variation of the damping coefficient of the normal force,  $C_{zq} + C_{z\dot{\alpha}}$  in Figure 19.

Comparison of the present dynamic test results with those obtained in other test facilities shows that the present curves are similar to those obtained previously with slight differences. However, it is observed that these differences become more important for values of  $\alpha$ , larger than  $25^0$ . It is seen that results are affected by the support system and flow characteristics of the tunnel. In order to eliminate the effect of support system in wind-tunnel experiments, wind-tunnel facilities should be improved to allow interference-free measurements of dynamic stability parameters over a large range of  $\alpha$  and  $\beta$ . The present day experimental test rigs are usually massive, which cause large flow blockage effects near or above the model. Artificial pressure fields resulting in vortex bursting and erroneous measurements can be observed due to this blockage effects. Therefore, the development of support-free magnetic suspension techniques for high-  $\alpha$  dynamic testing is of particular interest.

## REFERENCES

- [1] Avcı, S., May 2000, "Static and Forced Oscillatory Tests on a Generic Combat Aircraft Model in Ankara Wind Tunnel," M Sc. Thesis, Middle East Technical University, Ankara.
- [2] Altun, M., February 2001, "Manufacturing, Assembly and Commissioning of an Oscillating Test

Rig to Measure the Dynamic Stability Derivatives in the Ankara Wind Tunnel," M Sc. Thesis, Middle East Technical University, Ankara.

- [3] İyigün, I., March 2001, "Determination of Dynamic Stability Derivatives For a Generic Combat Aircraft Under Forced Oscillations," M Sc. Thesis, Middle East Technical University, Ankara.
- [4] Beyers, M.E., and Moulton, B. E., June 1984 "Pitch and Yaw Oscillation Experiments on the SDM at Mach 0.6," LTR-UA-76, Ottawa, Canada.
- [5] Guglieri, G., Quagliotti, F.B., May-June 1993, "Dynamic Stability Derivatives Evaluation in a Low-Speed Wind Tunnel," Journal of Aircraft, Volume 30, Number 3, pp. 421-423.
- [6] Guglieri, G., Quagliotti, F. B., Scarabelli, P. L., 1993, "Static and Oscillatory Experiments on the SDM at Politecnico di Torino," Nota Scientifica E Tecnica N. 74/93, Forced Oscillation Technique-Reference Documentation, vol.3, Politecnico di Torino, DIASP, Italy.
- [7] Ozdemir, E., 2000, "Calibration and Instrumentation of Ankara Wind Tunnel," M Sc. Thesis, Middle East Technical University, Ankara.
- [8] Orlik-Rückemann, K. J., "Subsonic Aerodynamic Coefficients of the SDM at Angles of Attack up to  $90^0$ , Report LTR-UA-93," Forced Oscillation Technique-Reference Documentation, vol.3, Politecnico di Torino, DIASP, Italy.

## ACKNOWLEDGEMENT

This work is supported by a grant from the Scientific and Technical Research Council of Turkey, TÜBİTAK, project MISAG 131.

This research is also supported by the support program of NATO-Research and Technology Organization, RTO, through project T-118. Both of these supports are gratefully acknowledged.

## VITA

### Mehmet ALTUN

He was born in Konya, Turkey. He graduated from Maltepe Military High School in Izmir, in 1991 and Air Force Academy in Istanbul, in 1995 respectively. He worked as a maintenance officer in 5<sup>th</sup> Air Force Base until September of 1998 in Merzifon, Turkey. He graduated from Middle East Technical University with a degree of M.Sc. in Aeronautical Engineering in 2001. After graduation he is assigned in Air Force



Academy, Aeronautical Engineering Department in Istanbul. He continues his Ph.D. studies in Istanbul Technical University, Aeronautical Engineering Department in Istanbul, Turkey.

**İbrahim İYİĞÜN**

He graduated from Istanbul Technical University, Aeronautical Engineering Department in 1994 in Istanbul. After graduation he worked in 2<sup>nd</sup> Air Supply and Maintenance Center until September of 1999 in Kayseri. He graduated from Middle East Technical University with a degree of M.Sc. in Aeronautical Engineering in 2001. After graduation he is assigned in Air Force HQ/Planning Department.